

Disentangling the role of microphysical and dynamical effects in determining cloud properties over the Atlantic

Ulrike Lohmann,¹ Ilan Koren,² and Yoram J. Kaufman³

Received 12 September 2005; revised 28 February 2006; accepted 31 March 2006; published 4 May 2006.

[1] MODIS satellite data reveal that over the Atlantic Ocean (20°S–30°N) in June–August 2002 indirect aerosol effects cause a decrease in the cloud top effective radius of stratiform clouds of 2.9 μm and an increase in cloud fraction of 21%, when increasing the aerosol optical thickness (AOT) from the cleanest 5 percentile to an AOT of 0.2. Thus, indirect aerosol effects are responsible for 72% (–8.8 W m^{-2}) of the –12.2 W m^{-2} decrease in the shortwave radiation at the top-of-the atmosphere (TOA). Global climate model simulations with and without indirect aerosol effects confirm a decrease in TOA shortwave cloud forcing of –9 W m^{-2} over the Atlantic from the cleanest to the highest AOT due to indirect aerosol effects. While MODIS shows an increase in cloud fraction due to aerosols, in the model aerosols cause primarily an increase in cloud water. Thus, unlike the analysis from MODIS, the increase in cloud fraction with increasing AOT is dominated by changes in dynamical regimes, not by aerosol indirect effects. **Citation:** Lohmann, U., I. Koren, and Y. J. Kaufman (2006), Disentangling the role of microphysical and dynamical effects in determining cloud properties over the Atlantic, *Geophys. Res. Lett.*, 33, L09802, doi:10.1029/2005GL024625.

1. Introduction

[2] The indirect aerosol effect of changing cloud albedo and cloud lifetime due to anthropogenic emissions of aerosols and their precursors has been evaluated from observational studies, starting with measurements in a giant expansion chamber [Gunn and Phillips, 1957], followed by ship track studies [King *et al.*, 1993] and lately also over continental areas [Feingold *et al.*, 2003; Penner *et al.*, 2004]. Investigations by Brenguier *et al.* [2000] and Schwartz *et al.* [2002] over the Atlantic Ocean showed that the cloud droplets are smaller in polluted clouds than in clean clouds. This contrast between polluted and clean clouds is, however, partially offset because the polluted clouds were thinner as they originated over the continents, which causes them to have a smaller liquid water path than their counterpart marine clean clouds. Since the cloud albedo depends on both the cloud droplet size and the cloud thickness these competing effects partially cancel each other making it more difficult to detect an indirect aerosol effect.

[3] Satellite data can also be used to understand some aspects of aerosol-cloud interactions. Suzuki *et al.* [2004],

for instance, showed that the aerosol number concentration decreases with increases in liquid water path because clouds with more water precipitate more frequently, thus removing more aerosols. Only if global models use an autoconversion rate that depends inversely on the cloud droplet number (which is a surrogate for the indirect cloud lifetime effect) can they counteract this effect and reproduce the observed near constancy of the liquid water path with increasing aerosol number concentration [Lohmann and Lesins, 2002; Quaas *et al.*, 2004; Suzuki *et al.*, 2004].

[4] New observations of aerosol effects on warm stratiform clouds over the North Atlantic from June to August 2002 were obtained by Kaufman *et al.* [2005]. They concluded that indirect aerosol effects of biomass burning and Saharan dust as compared to the clean marine base case with an AOT of 0.06 account for 72% of the –12.2 W m^{-2} decrease in the shortwave radiation at the top-of-the-atmosphere (TOA) in the region 20°S–30°N, which is mainly caused by increases in cloud fraction.

[5] Here we use the ECHAM4 general circulation model [Lohmann and Lesins, 2002] to disentangle the effects of meteorology and microphysics on changing cloud properties of warm stratiform clouds over the Atlantic in response to a higher aerosol optical depth and to study the global implications of aerosol effects on cloud fraction.

2. Model Description and Design of the Model Simulations

[6] The ECHAM4 general circulation model GCM [Roeckner *et al.*, 1996] used in this study is described in Lohmann and Lesins [2002]. Prognostic aerosol variables are the mass mixing ratios of sulfate, methane sulfonic acid, hydrophilic and hydrophobic organic carbon, hydrophilic and hydrophobic black carbon, sub- and supermicron dust, and sub- and supermicron sea salt. Transport, dry and wet deposition, and chemical transformations of the aerosols and gaseous precursors are calculated on-line with the GCM [Feichter *et al.*, 1996]. The prognostic cloud variables are the mass mixing ratios of cloud liquid water and cloud ice and the number concentrations of cloud droplets and ice crystals, as described in Lohmann *et al.* [1999] and Lohmann and Kärcher [2002].

[7] The total number concentration of hydrophilic aerosols, that is used for cloud droplet activation at cloud base, is obtained by assuming an externally mixed aerosol. We convert the mass of each aerosol component into an aerosol particle number assuming a separate lognormal distribution with a fixed dry density, dry modal radius and geometric width for each type [Hess *et al.*, 1998]. The cloud droplet concentration at cloud base of stratiform clouds is obtained from the number of hydrophilic aerosols and the sum of the

¹Institute of Atmospheric and Climate Science, Zurich, Switzerland.

²Department of Environmental Sciences, Weizmann Institute, Rehovot, Israel.

³NASA Goddard Space Flight Center, Greenbelt, Maryland, USA.

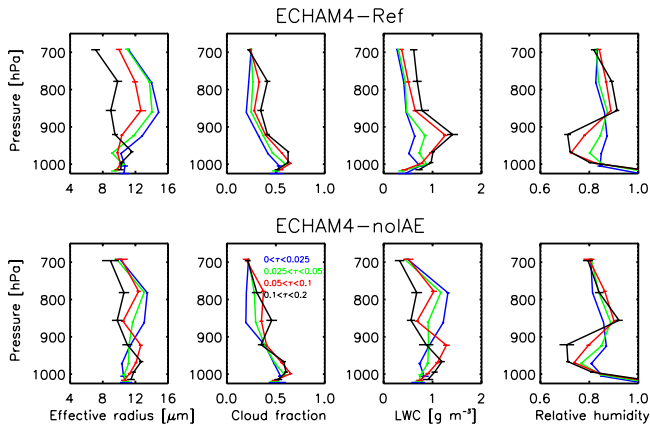


Figure 1. Cloud droplet effective radius, cloud fraction, in-cloud liquid water content (LWC) and relative humidity as a function of pressure over the Atlantic (30°N–20°S) from simulations (top) ECHAM-Ref and (bottom) ECHAM-noIAE during June, July and August. The cloud droplet effective radii and LWC are sampled only within the cloudy part of the grid box whenever clouds occur. All cases are limited to warm clouds with cloud top pressures larger 640 hPa with no overlying clouds for different bins of aerosol optical thickness (AOT). The horizontal bars refer to \pm one standard error.

grid mean vertical velocity and a turbulent contribution [Lohmann, 2002]. Cloud fraction is diagnosed from relative humidity [Roeckner *et al.*, 1996].

[8] All simulations were conducted in T30 horizontal resolution with 19 vertical levels and a 30 minute time-step. The reference simulation is the same as used in the study by Lohmann and Lesins [2002] (simulation ECHAM4-Ref) and was run over a period of 5 years after an initial spin-up of 3 months using climatological sea surface temperatures and sea ice extent. In the simulation ECHAM4-noIAE, that was run for 3 years, the indirect aerosol effect is turned off. Here the cloud droplet number concentration used for the cloud microphysics and radiation calculations is decoupled from the aerosol scheme. It is just a function of altitude, decreasing exponentially from 150 droplets cm^{-3} between the surface and 800hPa to 50 droplets cm^{-3} in the free atmosphere. Because the climate and the dynamics are comparable in the simulations ECHAM4-Ref and ECHAM-noIAE, we can attribute the differences between these two simulations to the indirect aerosol effect.

3. Results

[9] Kaufman *et al.* [2005] analyzed the stratiform cloud fraction and the cloud droplet effective radius at cloud top for the North Atlantic (5°N–30°N) and for the South Atlantic (20°S–5°N) for different AOT classes in $1^\circ \times 1^\circ$ grid boxes for which AOT can be simultaneously retrieved (<http://modisatmos.gsfc.nasa.gov>). These clouds were restricted to low level water clouds with cloud top pressures higher than 640 hPa with no overlying clouds. The average cloud top pressure is 870 hPa (1200 m) with a rather narrow distribution. The quantitative analysis in terms of aerosol-induced changes in cloud physical and radiative properties was then conducted by analyzing the change in cloud

properties between the 5th and 95th percentile for a logarithmic increase in aerosol optical thickness (AOT) from 0.02 to 0.44. We applied the same analysis for the same regions to the 12-hourly ECHAM4 data for June, July, August from all years, but limited ourselves to values in AOT below 0.2 in order to still have sufficient data in the largest AOT bin.

[10] As shown in Figure 1, in both simulations the effective radius decreases with increasing AOT but for different reasons. In ECHAM4-Ref, the liquid water content within the cloudy part of the grid box sampled only over cloudy events (LWC) increases with increasing AOT which, for a constant cloud droplet number concentration, would increase the effective radius. Thus the decrease in effective radius with increasing AOT is caused by the higher number of cloud droplets associated with higher AOT values, that is by, the indirect aerosol effect [see Kaufman *et al.*, 2002; Lohmann and Lesins, 2002].

[11] On the other hand, if no aerosol effects on clouds are included, that is, if the cloud droplet number concentration is only a function of altitude as in ECHAM4-noIAE, then LWC decreases with increasing AOT mimicking the decrease in effective radius with increasing AOT. This agrees with the results by Suzuki *et al.* [2004], that in the absence of the indirect aerosol effect, a high LWC implies more wet scavenging of aerosol particles, thus reducing AOT. In order to shift from the decrease in LWC with increasing AOT in ECHAM-noIAE to the increase in LWC with increasing AOT in simulation ECHAM4-Ref, the indirect aerosol effect has to overcompensate the higher wet removal rate at higher LWCs.

[12] In trying to disentangle the microphysical from the dynamical effect, changes in cloud top effective radius from the smallest to highest AOT bin can be analyzed. The change in cloud top effective radius over the Atlantic from the lowest to the highest AOT bin amounts to $-1.9 \mu\text{m}$ in ECHAM4-Ref but to $+0.2 \mu\text{m}$ in ECHAM-noIAE (Figure 2), that is, aerosol-induced changes are solely responsible for the decrease in the effective radius with increasing AOT. This aerosol-induced reduction in cloud droplet size in ECHAM4-Ref is in qualitative agreement with the MODIS data, but only amounts to 2/3 of the observed decrease over the same AOT range (Figure 2). In agreement with theory [Albrecht, 1989] and with the MODIS data [Kaufman *et al.*, 2005], the in-cloud liquid water content increases with increasing AOT when aerosol-cloud effects are included as in simulation ECHAM4-Ref but remains constant in the absence of these.

[13] In both simulations the cloud fraction increases from the lowest to the highest AOT bin by 0.29 to 0.34 (Figure 2), which is larger than the observed increase in cloud fraction of 0.21 [Kaufman *et al.*, 2005]. More importantly, whereas the MODIS data relate the cloud fraction increase mainly to aerosol indirect effects, the model suggests that it is dominated by dynamical changes as the increase in cloud fraction with increasing AOT in ECHAM4-noIAE amounts to 85% of the increase in simulation ECHAM4-Ref. The boundary layer structure is distinctly different for the low and high AOT cases such that during low AOT cases the relative humidity is more uniform with altitude, while it shows an inversion for the high AOT cases being more moist above 900 hPa (Figure 1).

[14] The shortwave radiation at the surface decreases with increasing AOT in both simulations. This decrease in the ECHAM4-noIAE simulation is caused primarily by the higher cloud fraction in the higher AOT case. It is enhanced by almost 70% due to aerosol indirect effects in simulation ECHAM4-Ref as compared to simulation ECHAM-noIAE (Figure 2). The TOA shortwave radiation, however, increases in both simulations as a results of the different dynamic regimes. In the high AOT cases, the clear-sky absorption increases significantly due to lower cloud-top pressures (Figure 2), and hence more absorption by water vapor and absorbing aerosols above cloud top (see Figure 1 for higher relative humidity above 900 hPa). These effects are eliminated when the change in shortwave cloud forcing (defined as the difference between total sky and clear-sky conditions) is examined. Evaluating cloud forcing is also more directly comparable to the offline indirect aerosol effect calculations by *Kaufman et al.* [2005], which were conducted keeping all other parameters except the changes in cloud properties constant. The shortwave cloud forcing decreases by -13.4 W m^{-2} in ECHAM4-Ref but only by -4.8 W m^{-2} in ECHAM-noIAE. This means that -8.6 W m^{-2} are caused by indirect aerosol effects, which is in qualitative agreement with the -8.8 W m^{-2} due to indirect aerosol effects in the MODIS data [*Kaufman et al.*, 2005].

[15] To put these regional estimates into perspective, we redid this analysis globally from climate model output for an entire year (Figure 3). It reveals that globally the cloud

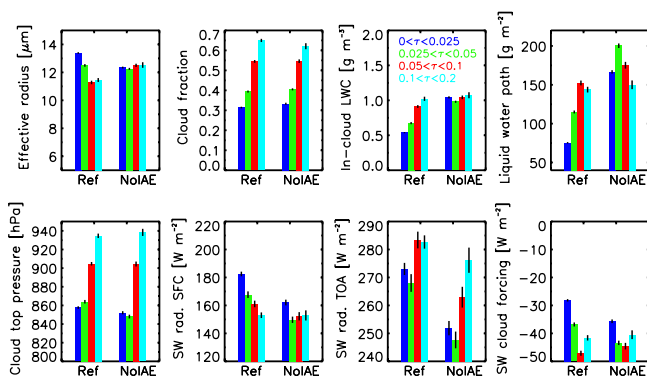


Figure 2. Cloud top effective radius, low-level cloud fraction assuming maximum overlap, in-cloud liquid water content (LWC) of warm clouds with cloud top pressures larger 640 hPa, total cloud liquid water path (LWP) obtained as vertical integral of the product of cloud fraction with LWC, cloud top pressure, net shortwave radiation (SW) at the surface (SFC), at the top-of-the-atmosphere (TOA) and the TOA shortwave cloud forcing over the Atlantic Ocean (20°S – 30°N) during June, July and August for simulations ECHAM4-Ref (Ref) and ECHAM4-noIAE (noIAE). As for Figure 1, the cloud droplet effective radii and in-cloud liquid water content are sampled only within the cloudy part of the grid box when clouds occur. The respective changes from the MODIS data in this region from the cleanest AOT (lowest 5 percentile) to an AOT of 0.2 (and to the highest AOT (95 percentile)) are: a decrease in cloud droplet radius of $-2.9 \mu\text{m}$ ($-4.1 \mu\text{m}$); an increase in cloud fraction of 0.21 (0.33); an increase in LWP of 9.4 g m^{-2} (14.8 g m^{-2}).

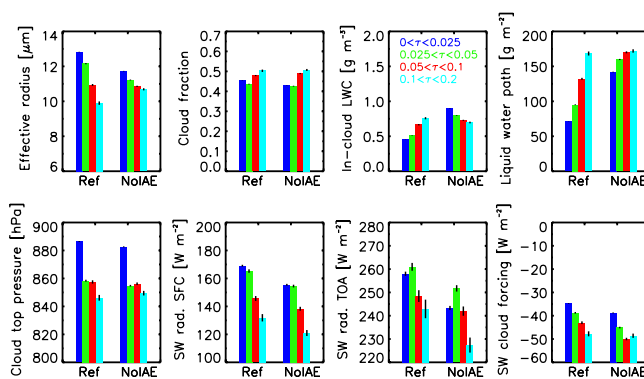


Figure 3. Same as Figure 2 but from model data over the entire globe from one full year.

top radius decreases by $2.9 \mu\text{m}$ in ECHAM4-Ref and by $1 \mu\text{m}$ in ECHAM-noIAE, that is, 65% of this decrease are caused by indirect aerosol effects. The increase in cloud fraction is more modest amounting to only 0.05 to 0.08 in ECHAM4-Ref and ECHAM4-noIAE, respectively, again dominated by dynamical changes. As over the Atlantic, LWC increases with increasing AOT in ECHAM-Ref but decreases with increasing AOT in ECHAM4-noIAE because of the increased wet scavenging rate at higher LWCs.

[16] The reduction in shortwave radiation at the top-of-the-atmosphere is rather similar in both experiments. Only if changes in the clear-sky are excluded by evaluating the shortwave cloud forcing instead, then there is a difference between the two simulations. The decrease in shortwave cloud forcing due to the increased cloud fraction and liquid water path in ECHAM4-noIAE amounts to -9.8 W m^{-2} . It is 3.1 W m^{-2} larger in simulation ECHAM4-Ref suggesting that 25% of the decrease in shortwave cloud forcing can be attributed to indirect aerosol effects.

[17] The global analysis helps to put the regional findings of MODIS into a global perspective. The simulations, however, suggest that differences in dynamical regimes are more important than aerosol indirect effects for the increase in cloud fraction and the decrease in shortwave cloud forcing with increasing AOT. These findings point to the need for improvements in GCMs in terms of turbulent mixing, aerosol activation, cloud dynamics, precipitation as well as for cloud resolving model simulations of aerosol-cloud interactions.

[18] **Acknowledgment.** We thank the anonymous reviewers for useful comments and suggestions.

References

- Albrecht, B. (1989), Aerosols, cloud microphysics, and fractional cloudiness, *Science*, *245*, 1227–1230.
- Brenguier, J.-L., H. Pawlowska, L. Schüller, R. Preusker, J. Fischer, and Y. Foucart (2000), Radiative properties of boundary layer clouds: Droplet effective radius versus number concentration, *J. Atmos. Sci.*, *57*, 803–821.
- Feichter, J., E. Kjellström, H. Rodhe, F. Dentener, J. Lelieveld, and G.-J. Roelofs (1996), Simulation of the tropospheric sulfur cycle in a global climate model, *Atmos. Environ.*, *30*, 1693–1707.
- Feingold, G., W. L. Eberhard, D. E. Veron, and M. Previdi (2003), First measurements of the Twomey indirect effect using ground-based remote sensors, *Geophys. Res. Lett.*, *30*(6), 1287, doi:10.1029/2002GL016633.
- Gunn, R., and B. B. Phillips (1957), An experimental investigation of the effect of air pollution on the initiation of rain, *J. Meteorol.*, *14*, 272–280.

- Hess, M., P. Koepke, and I. Schult (1998), Optical properties of aerosols and clouds: The software package OPAC, *Bull. Am. Meteorol. Soc.*, *79*, 831–844.
- Kaufman, Y. J., D. Tanré, and O. Boucher (2002), A satellite view of aerosols in the climate system, *Nature*, *419*, 215–223.
- Kaufman, Y. J., I. Koren, L. A. Remer, D. Rosenfeld, and Y. Rudich (2005), The effect of smoke, dust and pollution aerosol on shallow cloud development over the Atlantic ocean, *Proc. Natl. Acad. Sci. U. S. A.*, *11*, 207–11,212.
- King, M. D., L. F. Radke, and P. V. Hobbs (1993), Optical-properties of marine stratocumulus clouds modified by ships, *J. Geophys. Res.*, *98*, 2729–2739.
- Lohmann, U. (2002), Possible aerosol effects on ice clouds via contact nucleation, *J. Atmos. Sci.*, *59*, 647–656.
- Lohmann, U., and B. Kärcher (2002), First interactive simulations of cirrus clouds formed by homogeneous freezing in the ECHAM general circulation model, *J. Geophys. Res.*, *107*(D10), 4105, doi:10.1029/2001JD000767.
- Lohmann, U., and G. Lesins (2002), Stronger constraints on the anthropogenic indirect aerosol effect, *Science*, *298*, 1012–1016.
- Lohmann, U., J. Feichter, C. C. Chuang, and J. E. Penner (1999), Prediction of the number of cloud droplets in the ECHAM GCM, *J. Geophys. Res.*, *104*, 9169–9198.
- Penner, J. E., X. Dong, and Y. Chen (2004), Observational evidence of a change in radiative forcing due to the indirect aerosol effect, *Nature*, *427*, 231–234.
- Quaas, J., O. Boucher, and F.-M. Bréon (2004), Aerosol indirect effects in POLDER satellite data and the Laboratoire de Météorologie Dynamique-Zoom (LMDZ) general circulation model, *J. Geophys. Res.*, *109*, D08205, doi:10.1029/2003JD004317.
- Roeckner, E., et al. (1996), The atmospheric general circulation model ECHAM4: Model description and simulation of the present day climate, *Tech. Rep. 218*, Max-Planck-Inst. für Meteorol., Hamburg, Germany.
- Schwartz, S. E., Harshvardhan, and C. Benkovitz (2002), Influence of anthropogenic aerosol on cloud optical depth and albedo shown by satellite measurements and chemical transport modeling, *Proc. Natl. Acad. Sci. U. S. A.*, *99*, 1784–1789.
- Suzuki, K., T. Nakajima, A. Numaguti, T. Takemura, K. Kawamoto, and A. Higurashi (2004), A study of the aerosol effect on a cloud field with simultaneous use of GCM modeling and satellite observations, *J. Atmos. Sci.*, *61*, 179–194.

Y. J. Kaufman, NASA Goddard Space Flight Center, Greenbelt, MD 20771, USA.

I. Koren, Department of Environmental Sciences, Weizmann Institute, P.O. Box 26, Rehovot 76100, Israel.

U. Lohmann, Institute of Atmospheric and Climate Science, ETH Zurich, 8092 Zurich, Switzerland. (ulrike.lohmann@env.ethz.ch)